Developing wideband antenna based on the metamaterial and dielectric silicon load for THz spectrum

Sachin Sharma
IIMT University Meerut
Sepideh Ebrahimi
Islamic Azad University
Ferdows B. Zarrabi (Ferdows.zarrabi@yahoo.com)
Islamic Azad University

Research Article

Keywords: Antenna, wireless communication, Terahertz, metamaterial

Posted Date: August 21st, 2023

DOI: https://doi.org/10.21203/rs.3.rs-3209512/v1

Additional Declarations: No competing interests reported.

Abstract

THz antenna with wide bandwidth and high Q-factor is interesting for various application including 6G application and THz sensing and controlling the surface current of the antenna is known as a technique for bandwidth enhancement. The slot antenna with metasurface is a good candidate for this aim. In this research, we have suggested a multilayer slot antenna with metamaterial load to provide wide bandwidth which covers the 0.38 to 0.57 THz with bandwidth of 40%. The metamaterial loads make various paths for the current on the surface of the antenna that makes possible achieving the wider bandwidth. The proposed antenna has gain of 4 dBi. To achieve higher bandwidth the dielectric silicon (Si) load is placed over the metasurface. The result shows that the height and form of the Si element can impact the bandwidth of the antenna. To modify the results of the antenna, the shape, height and width of the dielectric load over the antenna is examined. The antenna bandwidth is enhanced more than 100% and it covers 0.371 to 0.616 THz with 49% bandwidth. The proposed antenna is simulated with full wave time domain technique of FIT (finite integrated technique).

I. Introduction

Terahertz electromagnetic waves, with frequencies ranging from 0.1 to 10 THz and wavelengths spanning 0.03 to 3 mm, have garnered significant interest for their diverse applications [1]. The IEEE standard defines the THz wave within the 0.3–10 THz range [2]. Leveraging the unique properties of THz waves, various benefits have emerged: (1) Low Damage Potential: The energy of a single photon in the THz range is significantly lower than that of X-rays, making it safer for use in biomedical fields [3]. For instance, THz waves show promise in early skin cancer detection without causing harm to living organisms [4]. (2) High Spectral Resolution and Analysis: THz radiation's spectrum analysis is crucial for detecting hazardous substances like viruses, explosives, firearms, and chemicals [5, 6]. Its high spectral resolution enables precise identification and characterization of such materials [7]. (3) Penetration of Non-Metallic Materials: THz waves can penetrate certain non-metallic or non-polar materials due to their short wavelengths [8]. This capability allows for the scanning and imaging of otherwise opaque objects, resulting in higher definition images [9]. Consequently, THz waves find wide-ranging applications in sensing and security, including full-body scanners at airports [10]. (4) Expanded Bandwidth: As current spectrum resources face serious scarcity, antennas are being designed for higher frequency bands [11]. The THz band offers higher bandwidth potential, making active antennas in the THz range a preferred choice over traditional antennas [12]. This increased bandwidth facilitates faster data transmission and improved wireless communication systems [13].

Furthermore, the potential of THz waves extends beyond the mentioned applications. THz spectroscopy finds use in identifying molecular structures and interactions [14], benefiting fields such as chemistry and biology [15]. In satellite communication, THz technology has been considered for the satellite communication like the 6G services [16]. Researchers continue to explore novel applications, making THz technology an exciting and rapidly advancing area of research such as 6G application for high speed

communication [17]. As technology evolves and challenges are overcome, the widespread adoption of THz waves is expected to revolutionize various industries and scientific domains [18].

Terahertz (THz) antennas are vital devices for transmitting and receiving THz electromagnetic waves in emerging THz systems, offering small size, wide bandwidth, and high data rates [19 ,20]. However, their effectiveness is hindered by relatively high losses and challenges in fabrication accuracy due to their small size in the high-frequency THz bands. Nevertheless, researchers have made significant progress in overcoming these weaknesses and have developed various types of antennas over the past decade [21]. Recent research has focused on advancements in THz photoconductive antennas [22], THz horn antennas [23], THz lens antennas [24], THz microstrip antennas [25], and THz on-chip antennas [26].

In addition, Metamaterials, artificial structures with unique electromagnetic properties, have found extensive use across various spectra, including microwave [27], THz [28], and optic [29]. These materials possess negative permittivity and permeability, exhibiting a left-hand characteristic [30]. In the microwave range, metamaterials have been applied in diverse applications, such as filter design [31], CRLH circuits [32], gain enhancement [33], and polarization variation [34]. In the THz and optical spectrum, they have been harnessed as metasurfaces for chiral applications [35] and medical sensing, particularly in cancer detection [36].

Moreover, the dielectric resonator antenna (DRA) is known as a type of antenna that utilizes a dielectric material with a high permittivity to resonate at specific frequencies [37]. The dielectric material is typically shaped as a cylinder or other geometrical structures, which supports resonant modes, depending on its dimensions and permittivity [38]. When excited with an electromagnetic wave, the DRA stores energy in the form of electromagnetic fields within the dielectric material, causing it to resonate at its natural frequencies [39]. DRAs are commonly used in wireless communication systems, satellite communications, and other applications where compact size and high efficiency are essential [40].

In this research, we propose a novel multilayer slot antenna with a metamaterial load to achieve a wide bandwidth spanning the range of 0.35 to 0.58 THz. By incorporating metamaterial loads, we create various paths for the surface current, enabling the antenna to achieve the desired bandwidth enhancement. To further enhance the bandwidth, a dielectric silicon (Si) load is strategically placed over the metasurface. Through comprehensive simulations using the finite integrated technique (FIT) in the full-wave time domain, we investigate the impact of the height and form of the Si element on the antenna's bandwidth. The results reveal that the proposed modifications lead to a remarkable increase in bandwidth, surpassing 100%, and now covering an extended frequency range from 0.3 to 0.8 THz. our research contributes to the development of THz antennas with wide bandwidth and improved performance, making them suitable for various advanced applications, such as high-speed communication and high-resolution THz sensing. The simulation results validate the efficacy of our proposed design and underscore the potential of metamaterial-based techniques in achieving enhanced antenna performance for THz applications.

II. The antenna design and background theory

Slot Antenna theory

The cut off frequency for the microstrip slot antenna can be determined by the dimension of the slot and the permittivity of the substrate. Here, “c” is the speed of the light, “d” is the diameter of the slot and “ε_r” is the dielectric’s permittivity [41].

$$f = \frac{c}{2d\sqrt{\varepsilon_r}}$$

1

Based on the Eq. 1, the dimension of the aperture can be determined for the 0.5 THz, the dimension of the aperture should be around 200 µm and as a two layer structure it is assumed 180 µm for the proposed antenna.

ii. Antenna designing

The proposed antenna is presented in Fig.1 which is designed based on the slot antenna and coupled antenna. This antenna is multilayer antenna and designed 2 layers. The Roger RT5880Lz with permittivity of 2.2 without loss is used for both substrates layer with the thickness of 10µm for each layer. The total dimension of the substrate is 300×300µm^2. For 50Ω matching, the width of the transmission line over the RO5880 with thickness of 20 µm is obtained 6.5 µm and the length of the transmission line should be 109 µm or about of λg/2 where the $\lambda_g = \lambda/\sqrt{\varepsilon_r}$. Here, the feed line is placed on the bottom layer and length of the feed line is 150 µm as about 90µm of the feed line is pinpointed under the aperture and the width is supposed 10µm. Here, the thickness of the gold for metal layers is 0.02 µm. The CST microwave studio is utilized for simulation of the

Figure 1 The geometry of the proposed antenna with metasurface layer and all dimensions of the antennas are : L = 300µm, L_1 = 50µm, L_2 = 90µm, L_3 = 180µm, L_4 = 50µm

In the Fig. 2, three steps of design of the proposed antenna are presented. In the First step, a microstrip THZ antenna based on coupled with multilayer formation. For the first step (Step 1) and the metasurface is added in the 2nd step with the 4 rectangular element on each corner (Step 2) and finally the gaps as shown in Fig. 2 (c) is implemented to provide wide bandwidth as the 3rd step (Step 3).

Figure 2 Three steps of design the proposed antenna for THz application (a) 1st step of design as simple slot antenna (b) 2nd step by adding the metasurface (c) The 3rd step by implementing the gaps

iii. Predicable fabrication process

In the field of micro-fabrication, processes are carried out with the help of which miniature structures and devices with micro and nano dimensions are produced. This important technology is used in many industries such as electronics, optics, biotechnology, sensors, nanotechnology and solar cells. There are various methods for micro-fabrication, but one of the most important and widely used techniques is the so-called "production of silicon on insulator" or SOI (Silicon on Insulator). In this method, a thin layer of silicon as an active material is placed on an insulating layer. This technology is very useful for manufacturing integrated circuits, sensors, nano machines and other precision structures [42–43].

Micro-fabrication processes generally include the following steps:

1. Lithography (optical printing): This step involves covering a thin layer of light-sensitive material on the surface of the solution. Then a desired pattern is created on this layer so that the areas that are sensitive to minerals and semiconductors remain open.
2. Etching: In this step, using etching techniques, the unwanted parts of the thin layer are removed from the surface.
3. Deposition: New layers of material are added to the surface. These materials can be semiconductors, minerals, insulators or metals.
4. Doping: This step involves adding specific ions to the surface to create semiconducting properties in the micro-fabricated piece.
5. Annealing: At the end of the process, the produced structure is stabilized by performing steps of heat.

Micro-fabrication technology is structurally very complex and provides the ability to produce components with high precision, which is of great importance, especially in the fields of innovation and future technologies. This technology has important applications, especially in the industries related to electronics and communication, and causes significant improvements in these fields.

On the other hand in micro-fabrication, the bonding process is an important step that allows two parts to be connected together permanently including making multilayer structure and dielectric resonator antenna in the THz spectrum . This process strengthens the connection of the parts by creating a molecular connection between them, and allows the parts to be integrated and work better. Depending on the needs and materials used, the bonding process can be done by thermal bonding, adhesive bonding, or pressure bonding [44-45].

The bonding process in micro-fabrication generally includes the following steps:

1. Surface preparation: First, the surface of the parts to be bonded must be prepared. This includes cleaning the surface, removing pollutants and contamination, as well as arranging it in the desired shape and dimensions.
2. Selection of materials: The materials used for bonding must be suitable for the type of parts and final applications. Some types of materials used include adhesives, thermal adhesives, bonding films and various alloys.
3. Performing the bonding process: In this step, the parts are glued together and the connection process is done. If thermal bonding is used, the parts are brought together and then a connection is made between them using heat and pressure. In bonding, the appropriate glue is placed between two parts and a permanent connection is created by heat and pressure.
4. After bonding: After the bonding process is completed, the parts are well stabilized and can function as a complete unit. From now on, the joints resulting from bonding must support quality checks and components that can change depending on the application of the parts.

The bonding process in micro-fabrication creates tight and precise connections between parts, which is of great importance for nano and micro applications. This process illuminates the possibility of manufacturing and producing complex components and structures in miniature and nano dimensions and plays a key role in the progress of various industries including electronics and nanotechnology.

III. Discussions and Results of the antenna

The return loss of the three design steps was compared, and the results are illustrated in Fig. 3. The analysis demonstrates that the basic antenna exhibits a lower bandwidth, spanning from 0.35 to 0.45 THz, with a reflection value of -14 dB. Upon adding the metamaterial load in the second antenna, a noticeable impact on the return loss frequency and reflection value is observed. In this configuration, the antenna shows a dual band response at 0.55 and 0.7 THz, achieving a minimum reflection value of -31 dB. While the dual band response may be of interest in certain studies, it can potentially pose challenges, such as noise, in radar and satellite communication applications. The use of additional filters becomes necessary to mitigate these issues, albeit at an increased cost to the system. Consequently, combining a filter with the antenna proves to be advantageous. In the third step of the design, by introducing gaps in the outer ring of the metamaterial, the second resonance is effectively suppressed. As a result, the antenna exhibits a single resonance with a significantly wider bandwidth, spanning from 0.4 to 0.55 THz, and achieves a minimum reflection of -32 dB. This third configuration strikes a balance between improved performance and reduced complexity, making it a promising solution for various applications.

The antenna patterns for the three design steps are presented in Fig. 4, and their gains are compared at their respective resonances. The first antenna's gain and 2D pattern are displayed in Fig. 4(a) for 0.42 THz, with an antenna gain of approximately 4.02 dB and an impressive total efficiency of 99%. Moving on to the second antenna, Fig. 4(b) illustrates its gain of 4.52 dB at 0.56 THz, while maintaining a total efficiency of 94%. Finally, Fig. 4(c) depicts the third antenna's gain, which is 3.99 dB at 0.50 THz,

accompanied by a total efficiency of 95%. Notably, all the antenna radiation patterns exhibit a bi-directional pattern at theta = 0º and 180º, offering consistent and reliable coverage in multiple directions. The achieved gains and efficiency values demonstrate the effectiveness and performance of each design step.

The surface current distributions of the proposed antenna for the three design steps are illustrated in Fig. 5. In Fig. 5(a), the current distribution of the antenna in the first step is depicted, showing that the maximum current is concentrated along the feed line and at the edges of the rectangular aperture. As we progress to the 2nd and 3rd steps, as shown in Fig. 5(b) and Fig. 5(c) respectively, the maximum current now occurs on the split ring element.

Furthermore, it is observed that the maximum current of the antenna has undergone a significant increase in the 2nd and 3rd steps. Specifically, for the third antenna, the maximum current has risen from 2812 A/m to 3803 A/m, demonstrating the enhancement achieved through the optimization process in these design steps. The current distributions in the three steps provide valuable insights into the behavior of the antenna and the effect of metamaterial loading. The localization of the maximum current on the split ring element in the latter steps indicates the importance of this structure in achieving improved performance.

IV. Dielectric antenna design

To design the DRA (Dielectric Resonator Antenna), a dielectric element made of Si material is introduced above the aperture. As mentioned earlier, various parameters, including the height, shape, and width of the dielectric load element, can significantly impact the antenna's performance. In Fig. 6, the dielectric load is assumed to have a cylindrical shape with a rectangular cross-section, and two different parameters, the width and height of the dielectric, are investigated.

Figure 6(a) presents the examination of the width of the dielectric with values of 100, 140, and 180 μm. As depicted, increasing the width can lead to the creation of a multiband structure. For example, when the width is set to 180 μm, the antenna exhibits resonances at 0.25, 0.29, 0.32, and 0.6 THz. This shows the potential of achieving multiple resonance frequencies by appropriately adjusting the width of the dielectric element.

On the other hand, the height of the dielectric is studied as the second parameter, while maintaining the width (W_d) at 100 μm. The results are presented in Fig. 6(b) for rectangular dielectric elements with heights of 20, 30, and 40 μm. Surprisingly, the height of the dielectric does not appear to have any significant effect on the bandwidth of the antenna. This finding suggests that the antenna's bandwidth can be maintained or adjusted independently of the height parameter.

The shape of the dielectric element is another crucial parameter that significantly influences the performance of the antenna. In this investigation, three different shapes of rectangular, cylindrical, and cross elements are examined for the dielectric load, as depicted in Fig. 7(a). The width (W_d) is set at 100

μm for all shapes. For the cylindrical shape, a diameter of 100 μm is selected, and this value is used for the main arm of the elliptical in the cross element. Figure 7(b) presents the comparison of the three shapes in terms of their bandwidth and resonance characteristics. The cross elliptical element demonstrates the widest bandwidth, covering a range from 0.371 to 0.616 THz, with a bandwidth of 49% at 0.50 THz. In addition to its wide bandwidth, the cross element effectively removes higher harmonics and resonances present in the proposed antenna's frequency spectrum. The rectangular shape shows a multiband response with resonances at 0.35 THz (covering 0.316 to 0.381 THz), 0.46 THz, and 0.61 THz. Meanwhile, the cylindrical shape also exhibits a multiband characteristic, with the first resonance covering a range from 0.335 to 0.4755 THz. In brief, the investigation of different dielectric element shapes reveals that the cross elliptical element provides the widest bandwidth and effectively suppresses higher harmonics and resonances in the studied frequency spectrum. The selection of the appropriate shape is crucial for achieving desired bandwidth and resonance characteristics in the DRA antenna.

The electric field distribution inside of the dielectric is presented in Fig. 8 for two different planes of the X-Z and Y-Z. The dielectric load makes hybrid mode of HEM [46].

The 2D pattern of the antenna with dielectric load for 0.55 THz is presented in Fig. 9. The antenna gain is increased up to 4.45 dB or in other words, it shows 0.5 dB enhancement in comparison the antenna without dielectric load. In the antenna without the dielectric load, the front to back ratio is 0 dB but for the antenna with load it is increased up to 1.2 dB.

The last factor is the permittivity of the dielectric and here the return loss is examined for Ro-5880 with permittivity of 2.2, Pyrex with permittivity of 4.85 and silicon with permittivity of 11.9 and all these material are assumed as a lossless material (loss tangent of zero). As shown in Fig. 10, the higher permittivity of the silicon provides wider bandwidth in comparison with Ro-5880 and Pyrex.

V. Conclusion

The current study was focused on slot antenna for the THz spectrum with high efficiency. To enhance the antenna bandwidth the metasurface is placed over the slot which enhances the antenna bandwidth up to 40% and finally the dielectric load is added to it which increased the bandwidth of the antenna up to 49%. The load shape is investigated and the results prove that the elliptical cross element has better performance in comparison the rectangular and cylindrical element. Although the gain of antenna for the antenna with cross element increases only about of 0.5 dB, the front to back ratio for in comparison the antenna without load increase about 1.2 dB.

Declarations

Ethical Approval

“not applicable”

Competing interests

“The authors have no relevant financial or non-financial interests to disclose”

Authors' contributions

Sachin Sharma, Ferdows B. Zarrabi: Conceptualization, Data analyzing, Methodology, Formal analysis, Investigation, Resources, Software, Validation, Visualization, Writing-Original Draft. **Sepideh Ebrahimi**: Writing-review & editing, Supervision, Validation, Data certifying.

. **Funding**

There is no funding available.

Availability of data and materials

“not applicable”

Consent for Publications:

“All the authors of the manuscript mutually agree on submission and publication in the journal Consent to Participate Not Applicable”

Conflict of Interest:

The authors declare no conflict of interest

Acknowledgements:

“not applicable”

References

1. Poorgholam-Khanjari, Shima, Ferdows B. Zarrabi, and Saughar Jarchi. "Compact and wide-band Quasi Yagi-Uda antenna based on periodic grating ground and coupling method in terahertz regime." *Optik* 203 (2020): 163990.
2. Hajiyat, Zahraa RM, Alyani Ismail, Aduwati Sali, and Mohd Nizar Hamidon. "Antenna in 6G wireless communication system: Specifications, challenges, and research directions." *Optik* 231 (2021): 166415.
3. Sun, Yiwen, Ming Yiu Sy, Yi-Xiang J. Wang, Anil T. Ahuja, Yuan-Ting Zhang, and Emma Pickwell-MacPherson. "A promising diagnostic method: Terahertz pulsed imaging and spectroscopy." *World journal of radiology* 3, no. 3 (2011): 55.
4. Sun, Qiushuo, Edward PJ Parrott, Yuezhi He, and Emma Pickwell-MacPherson. "In vivo THz imaging of human skin: Accounting for occlusion effects." *Journal of biophotonics* 11, no. 2 (2018):

e201700111.

5. Lee, Kanghee, Hyun Joo Choi, Jaehyeon Son, Hyun-Sung Park, Jaewook Ahn, and Bumki Min. "THz near-field spectral encoding imaging using a rainbow metasurface." *Scientific Reports* 5, no. 1 (2015): 14403.
6. Martín-Mateos, Pedro, Dovilė Čibiraitė-Lukenskienė, Roberto Barreiro, Cristina de Dios, Alvydas Lisauskas, Viktor Krozer, and Pablo Acedo. "Hyperspectral terahertz imaging with electro-optic dual combs and a FET-based detector." *Scientific reports* 10, no. 1 (2020): 1-7.
7. Chi, Taiyun, Min-Yu Huang, Sensen Li, and Hua Wang. "17.7 A packaged 90-to-300GHz transmitter and 115-to-325GHz coherent receiver in CMOS for full-band continuous-wave mm-wave hyperspectral imaging." In *2017 IEEE International Solid-State Circuits Conference (ISSCC)*, pp. 304-305. IEEE, 2017.
8. Olivieri, Luana, Luke Peters, Vittorio Cecconi, Antonio Cutrona, Maxwell Rowley, Juan Sebastian Totero Gongora, Alessia Pasquazi, and Marco Peccianti. "Terahertz Nonlinear Ghost Imaging via Plane Decomposition: Toward Near-Field Micro-Volumetry." *ACS Photonics* (2023).
9. Xu, Zhimin, and Edmund Y. Lam. "Image reconstruction using spectroscopic and hyperspectral information for compressive terahertz imaging." *JOSA A* 27, no. 7 (2010): 1638-1646.
10. Shen, Xilin, Charles R. Dietlein, Erich Grossman, Zoya Popovic, and François G. Meyer. "Detection and segmentation of concealed objects in terahertz images." *IEEE transactions on Image Processing* 17, no. 12 (2008): 2465-2475.
11. Poorgholam-Khanjari, Shima, and Ferdows B. Zarrabi. "Dual-band THz antenna with SNG loads for biosensing and early skin cancer detection with Fano response: A numerical study." *Proceedings of the Institution of Mechanical Engineers, Part L: Journal of Materials: Design and Applications* 236, no. 11 (2022): 2326-2335.
12. Poorgholam-Khanjari, Shima, and Ferdows B. Zarrabi. "Reconfigurable Vivaldi THz antenna based on graphene load as hyperbolic metamaterial for skin cancer spectroscopy." *Optics Communications* 480 (2021): 126482.
13. Sadeghzadeh, Ramezan Ali, and Ferdows B. Zarrabi. "Metamaterial Fabry–Perot cavity implementation for gain and bandwidth enhancement of THz dipole antenna." *Optik* 127, no. 13 (2016): 5181-5185.
14. Baxter, Jason B., and Glenn W. Guglietta. "Terahertz spectroscopy." *Analytical chemistry* 83, no. 12 (2011): 4342-4368.
15. Plusquellic, David F., Karen Siegrist, Edwin J. Heilweil, and Okan Esenturk. "Applications of terahertz spectroscopy in biosystems." *ChemPhysChem* 8, no. 17 (2007): 2412-2431.
16. Tekbiyik, Kürşat, Güneş Karabulut Kurt, Alı Riza Ektı, and Halim Yanikomeroglu. "Reconfigurable intelligent surfaces empowered THz communication in LEO satellite networks." *IEEE Access* 10 (2022): 121957-121969.
17. De Alwis, Chamitha, Anshuman Kalla, Quoc-Viet Pham, Pardeep Kumar, Kapal Dev, Won-Joo Hwang, and Madhusanka Liyanage. "Survey on 6G frontiers: Trends, applications, requirements, technologies

and future research." *IEEE Open Journal of the Communications Society* 2 (2021): 836-886.

18. Martín-Mateos, Pedro, Dovilė Čibiraitė-Lukenskienė, Roberto Barreiro, Cristina de Dios, Alvydas Lisauskas, Viktor Krozer, and Pablo Acedo. "Hyperspectral terahertz imaging with electro-optic dual combs and a FET-based detector." *Scientific reports* 10, no. 1 (2020): 14429.
19. Sarieddeen, Hadi, Nasir Saeed, Tareq Y. Al-Naffouri, and Mohamed-Slim Alouini. "Next generation terahertz communications: A rendezvous of sensing, imaging, and localization." IEEE Communications Magazine 58, no. 5 (2020): 69-75.
20. Koenig, Swen, Daniel Lopez-Diaz, Jochen Antes, Florian Boes, Ralf Henneberger, Arnulf Leuther, Axel Tessmann et al. "Wireless sub-THz communication system with high data rate." Nature photonics 7, no. 12 (2013): 977-981
21. He, Yejun, Yaling Chen, Long Zhang, Sai-Wai Wong, and Zhi Ning Chen. "An overview of terahertz antennas." *China Communications* 17, no. 7 (2020): 124-165.
22. Burford, Nathan M., and Magda O. El-Shenawee. "Review of terahertz photoconductive antenna technology." *Optical Engineering* 56, no. 1 (2017): 010901-010901.
23. Aqlan, Basem, Mohamed Himdi, Laurent Le Coq, and Hamsakutty Vettikalladi. "Sub-THz circularly polarized horn antenna using wire electrical discharge machining for 6G wireless communications." *IEEE Access* 8 (2020): 117245-117252..
24. Lee, J. N., Y. K. Cho, J. H. Jung, and S. B. Hyun. "High-gain sub-terahertz lens horn antenna with a metal guide." *Electronics Letters* 56, no. 14 (2020): 689-691.
25. Zarrabi, Ferdows B., Mir Mohsen Seyedsharbaty, Zeeshan Ahmed, Afsaneh Saee Arezoomand, and Samaneh Heydari. "Wide band yagi antenna for terahertz application with graphene control." *Optik* 140 (2017): 866-872.
26. Balasekaran, Sundararajan, Kazuomi Endo, Tadao Tanabe, and Yutaka Oyama. "Patch antenna coupled 0.2 THz TUNNETT oscillators." *Solid-state electronics* 54, no. 12 (2010): 1578-1581.
27. Hossain, Amran, Mohammad Tariqul Islam, Gan Kok Beng, Saad Bin Abul Kashem, Mohamed S. Soliman, Norbahiah Misran, and Muhammad EH Chowdhury. "Microwave brain imaging system to detect brain tumor using metamaterial loaded stacked antenna array." *Scientific Reports* 12, no. 1 (2022): 16478.
28. Xu, Wendao, Lijuan Xie, and Yibin Ying. "Mechanisms and applications of terahertz metamaterial sensing: a review." *Nanoscale* 9, no. 37 (2017): 13864-13878.
29. Mobasser, Shohreh, Shima Poorgholam-Khanjari, Maryam Bazgir, and Ferdows B. Zarrabi. "Highly sensitive reconfigurable plasmonic metasurface with dual-band response for optical sensing and switching in the mid-infrared spectrum." *Journal of Electronic Materials* 50 (2021): 120-128.
30. Du John, H. Victor, Tony Jose, A. Amir Anton Jone, K. Martin Sagayam, Binay Kumar Pandey, and Digvijay Pandey. "Polarization insensitive circular ring resonator based perfect metamaterial absorber design and simulation on a silicon substrate." *Silicon* 14, no. 14 (2022): 9009-9020.
31. Yang, Wei, and Yu-Sheng Lin. "Tunable metamaterial filter for optical communication in the terahertz frequency range." *Optics Express* 28, no. 12 (2020): 17620-17629.

32. Mansouri, Zahra, Afsaneh Saee Arezoomand, Samaneh Heydari, and Ferdows B. Zarrabi. "Dual notch UWB fork monopole antenna with CRLH metamaterial load." *Progress In Electromagnetics Research C* 65 (2016): 111-119.
33. Devarapalli, Ananda Babu, and Tamasi Moyra. "Design of a metamaterial loaded W-shaped patch antenna with FSS for improved bandwidth and gain." *Silicon* 15, no. 4 (2023): 2011-2024.
34. Zarrabi, Ferdows B., Azadeh Pirooj, and Kioumars Pedram. "Metamaterial loads used in microstrip antenna for circular polarization." *International Journal of RF and Microwave Computer-Aided Engineering* 29, no. 10 (2019): e21869.
35. Ataloglou, Vasileios G., Michael Chen, Minseok Kim, and George V. Eleftheriades. "Microwave Huygens' metasurfaces: Fundamentals and applications." *IEEE Journal of Microwaves* 1, no. 1 (2021): 374-388.
36. La Spada, Luigi, Filiberto Bilotti, and Lucio Vegni. "Metamaterial biosensor for cancer detection." In *SENSORS, 2011 IEEE*, pp. 627-630. IEEE, 2011.
37. Varshney, Gaurav. "Tunable terahertz dielectric resonator antenna." *Silicon* 13, no. 6 (2021): 1907-1915.
38. Vishwanath, Gaurav Varshney, and Bikash Chandra Sahana. "Tunable terahertz circularly polarized dielectric resonator antenna with the higher order modes." *Silicon* (2021): 1-11.
39. Soren, Dipali, Rowdra Ghatak, Rabindra Kishore Mishra, and Dipak Poddar. "Dielectric resonator antennas: Designs and advances." *Progress In Electromagnetics Research B* 60 (2014): 195-213.
40. Petosa, A. M. M. A., Apisak Ittipiboon, Y. M. M. Antar, D. Roscoe, and M. Cuhaci. "Recent advances in dielectric-resonator antenna technology." *IEEE Antennas and Propagation magazine* 40, no. 3 (1998): 35-48.
41. Kazemi, Fatemeh. "High Q-factor compact and reconfigurable THz aperture antenna based on graphene loads for detecting breast cancer cells." *Superlattices and Microstructures* 153 (2021): 106865.
42. Hierlemann, Andreas, Oliver Brand, Christoph Hagleitner, and Henry Baltes. "Microfabrication techniques for chemical/biosensors. " *Proceedings of the IEEE* 91, no. 6 (2003): 839-863.
43. Bazgir, Maryam, Ferdows B. Zarrabi, Sanghoon Sim, and Kioumars Pedram. "The Nano aperture in optical regime for bio-sensing, metasurface, and energy harvesting application: Technical Review." *Sensors and Actuators A: Physical* (2023): 114495.
44. Mehra, Amit, Arturo A. Ayón, Ian A. Waitz, and Martin A. Schmidt. "Microfabrication of high-temperature silicon devices using wafer bonding and deep reactive ion etching." *Journal of Microelectromechanical Systems* 8, no. 2 (1999): 152-160.
45. Murozaki, Yuichi, Kousuke Nogawa, and Fumihito Arai. "Miniaturized load sensor using quartz crystal resonator constructed through microfabrication and bonding." *Robomech Journal* 1, no. 1 (2014): 1-7.
46. Sharma, Anand, Gourab Das, and Ravi Kumar Gangwar. "Dual-band dual-polarized hybrid aperture-cylindrical dielectric resonator antenna for wireless applications." *International Journal of RF and*

Microwave Computer-Aided Engineering 27, no. 5 (2017): e21092.

Figures

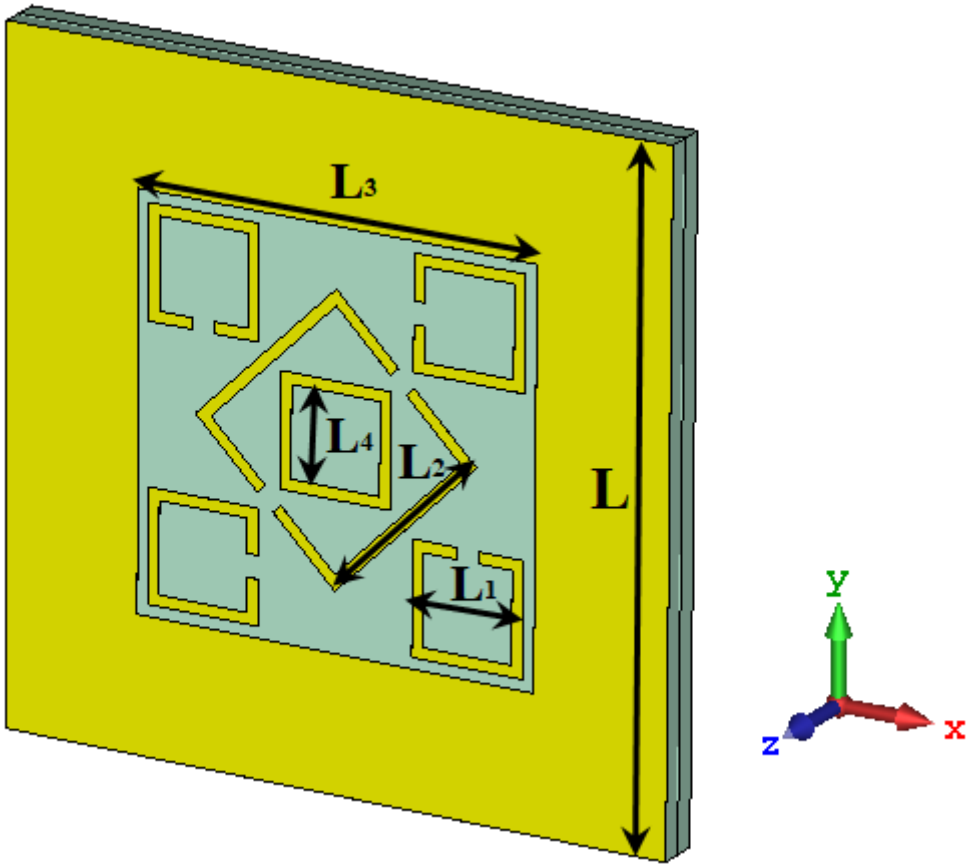

Figure 1

The geometry of the proposed antenna with metasurface layer and all dimensions of the antennas are : L = 300μm, L_1 = 50μm, L_2 = 90μm, L_3 = 180μm, L_4 = 50μm

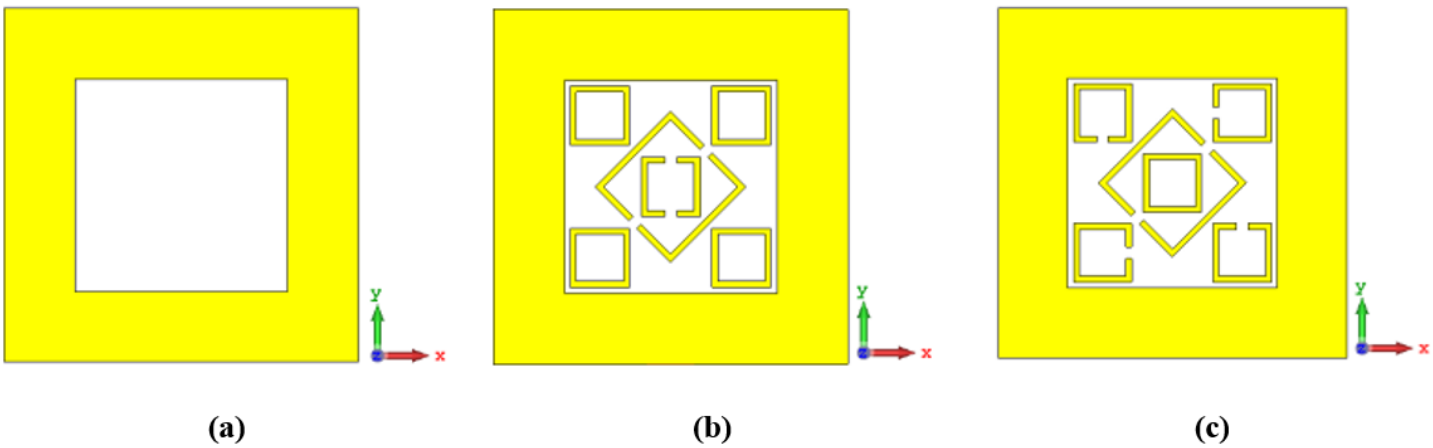

Figure 2

Three steps of design the proposed antenna for THz application (a) 1st step of design as simple slot antenna (b) 2nd step by adding the metasurface (c) The 3rd step by implementing the gaps

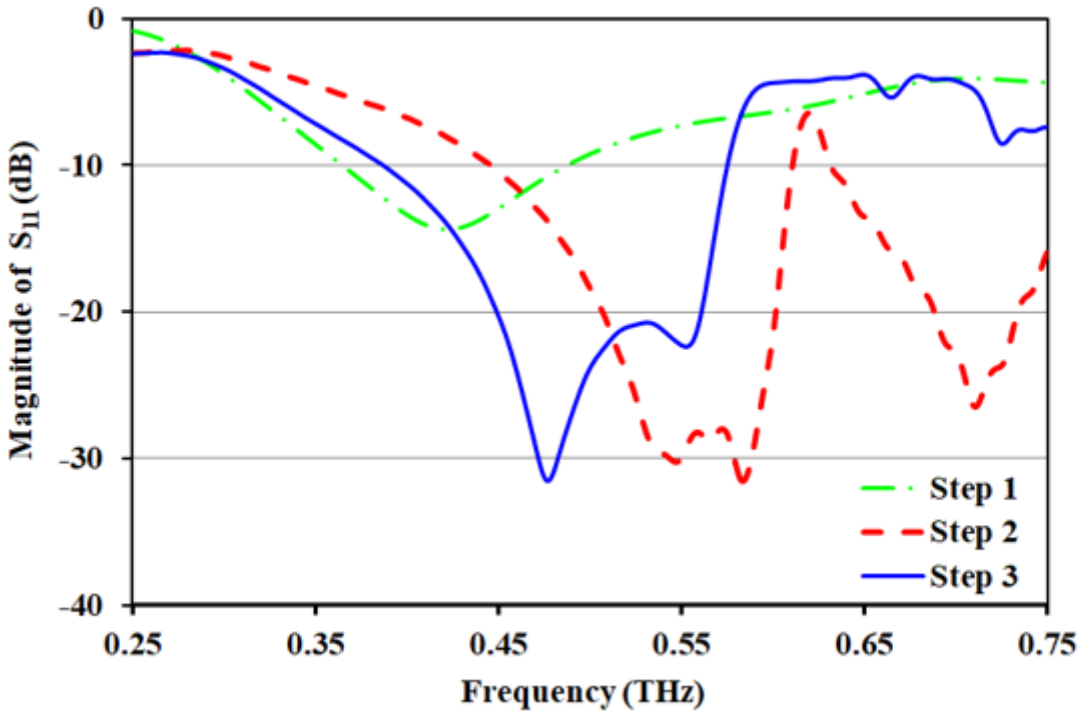

Figure 3

The antenna return loss for three steps of design

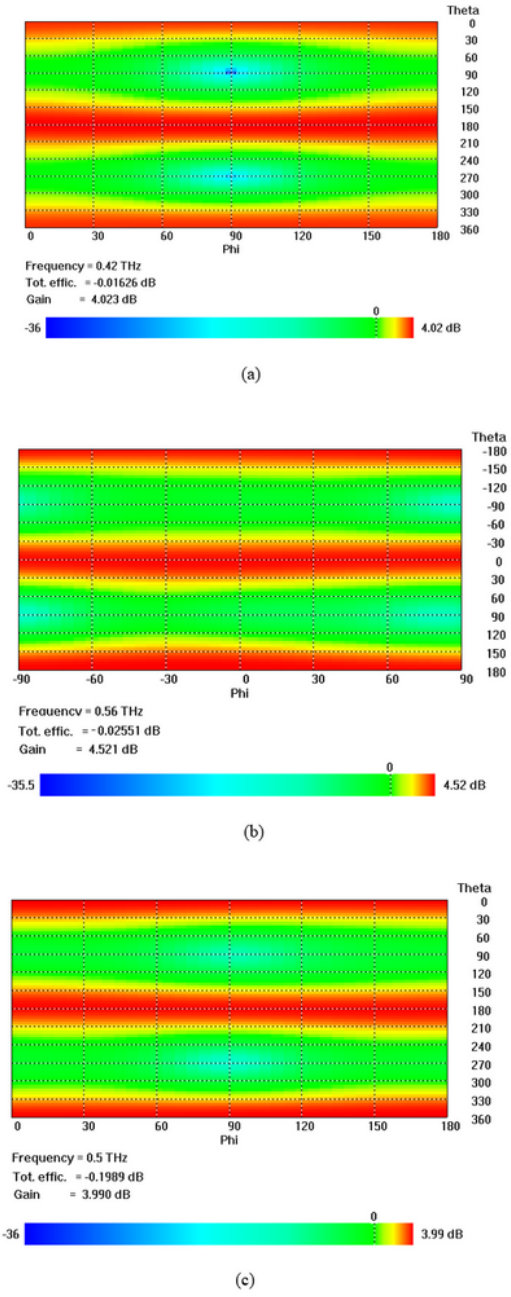

Figure 4

The antenna pattern for three steps (a) For the step 1 at 0.42 THz (b) For the step 2 at 0.56 THz (c) For the step 3 at 0.5 THz

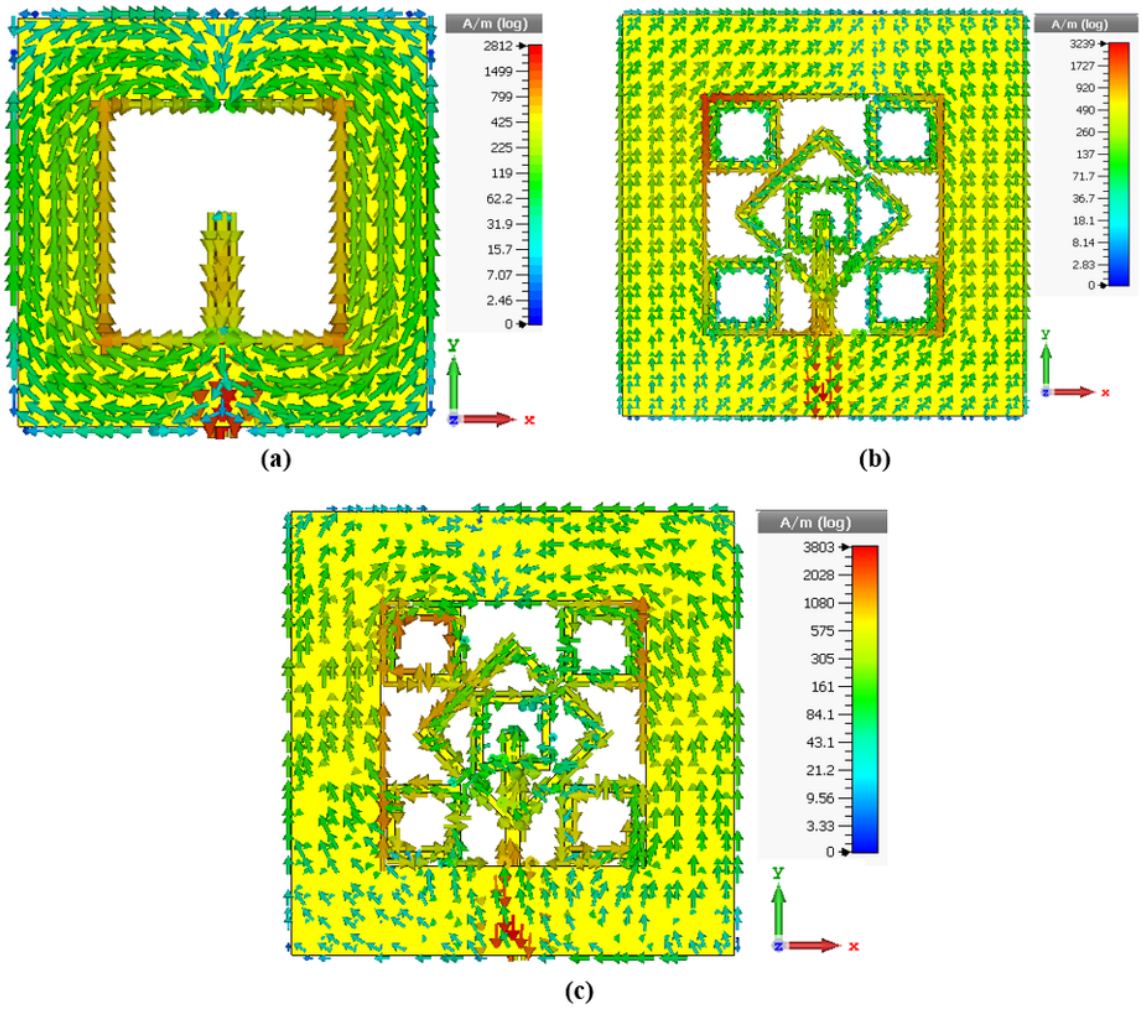

Figure 5

The surface current of 3 steps of the antenna designing and study the effect of the metasurface element.

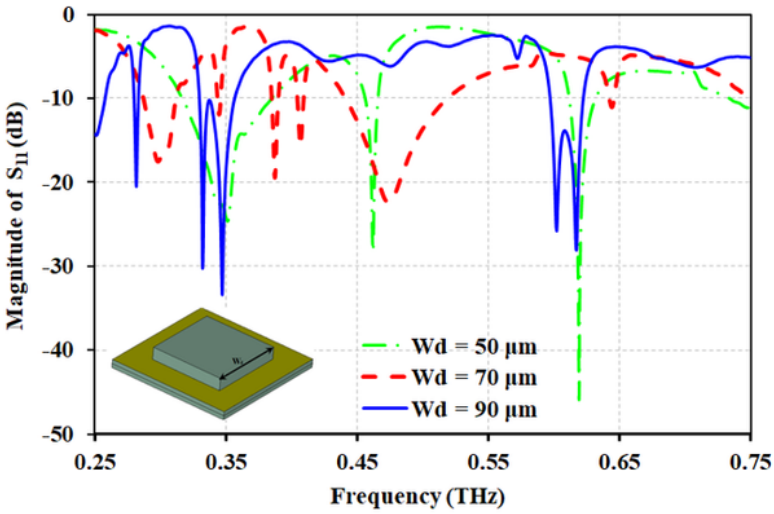

(a)

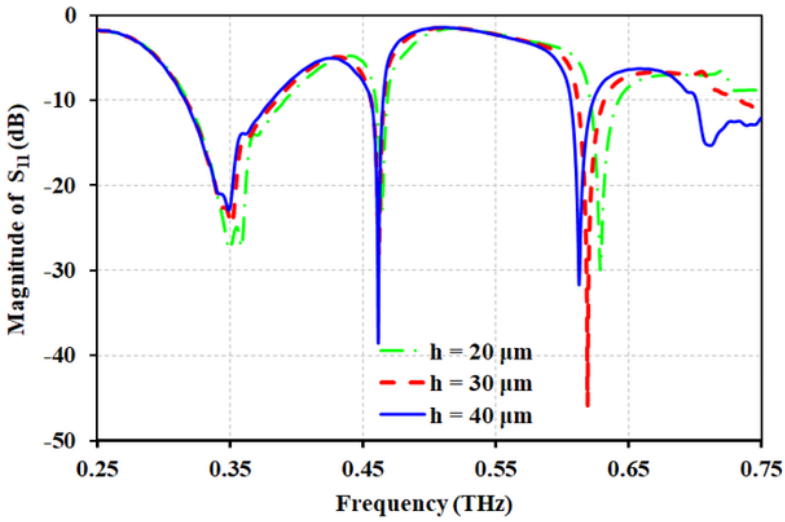

(b)

Figure 6

The return loss of the antenna with rectangular dielectric (a) Placing the rectangular dielectric over the aperture and checking of the W_d for 100 ,140 and 180 µm with the height of 20 µm (b) Study the effect of the height of the dielectric load with W_d = 100 µm.

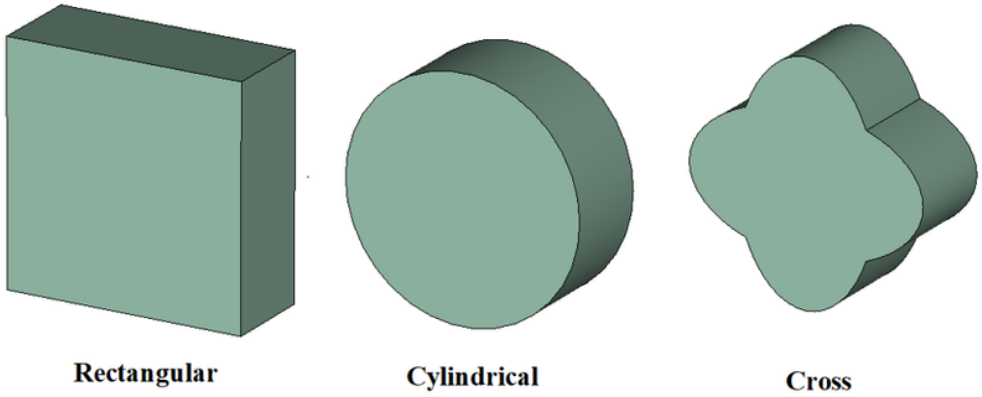

(a)

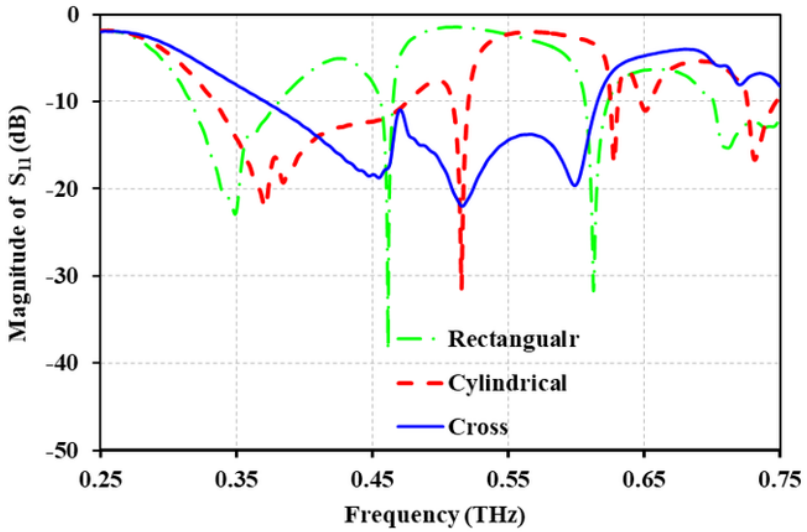

(b)

Figure 7

The various shapes of the dielectric load for the DRA (b) The return loss of the antenna for various shape of dielectric load

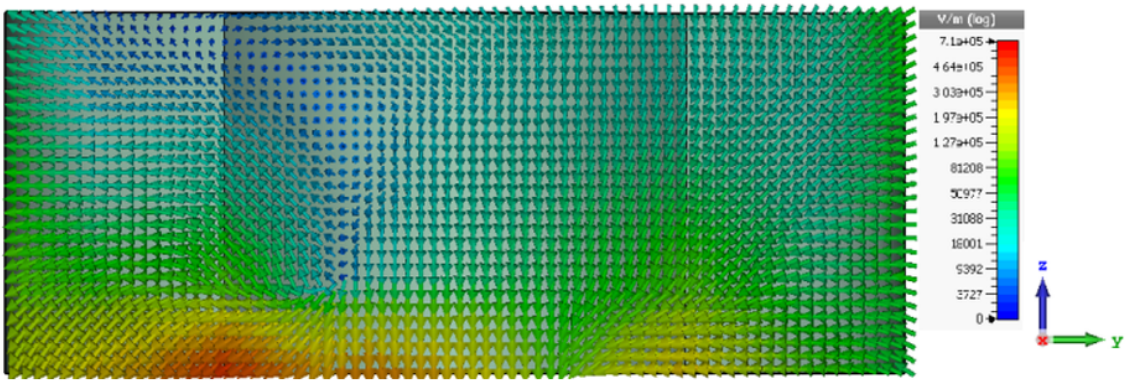

(a)

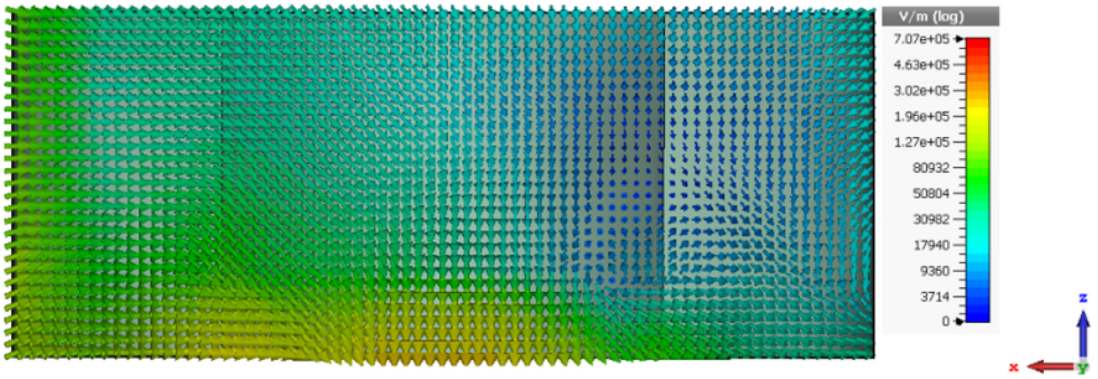

(b)

Figure 8

The electric field distribution inside of the dielectric (a) cutting in the Y-Z plane (b) cutting in the X-Z plane

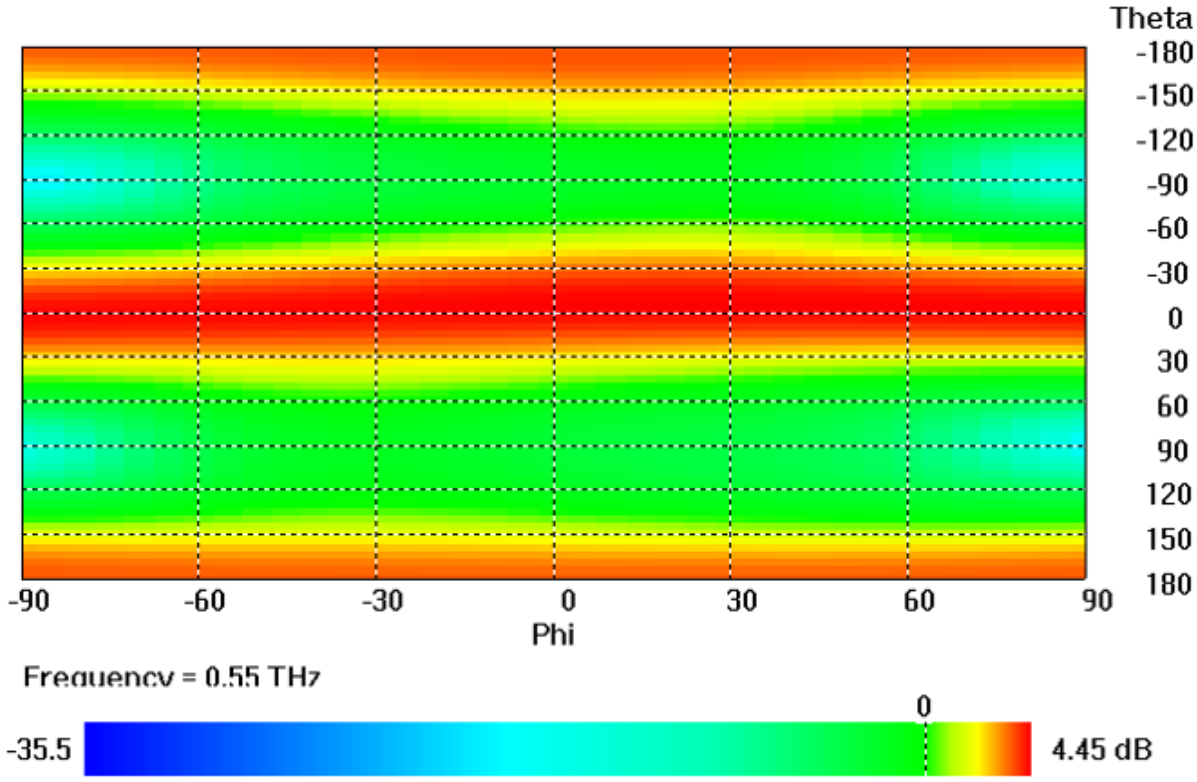

Figure 9

The radiation pattern of the antenna with dielectric load at 0.55 THz

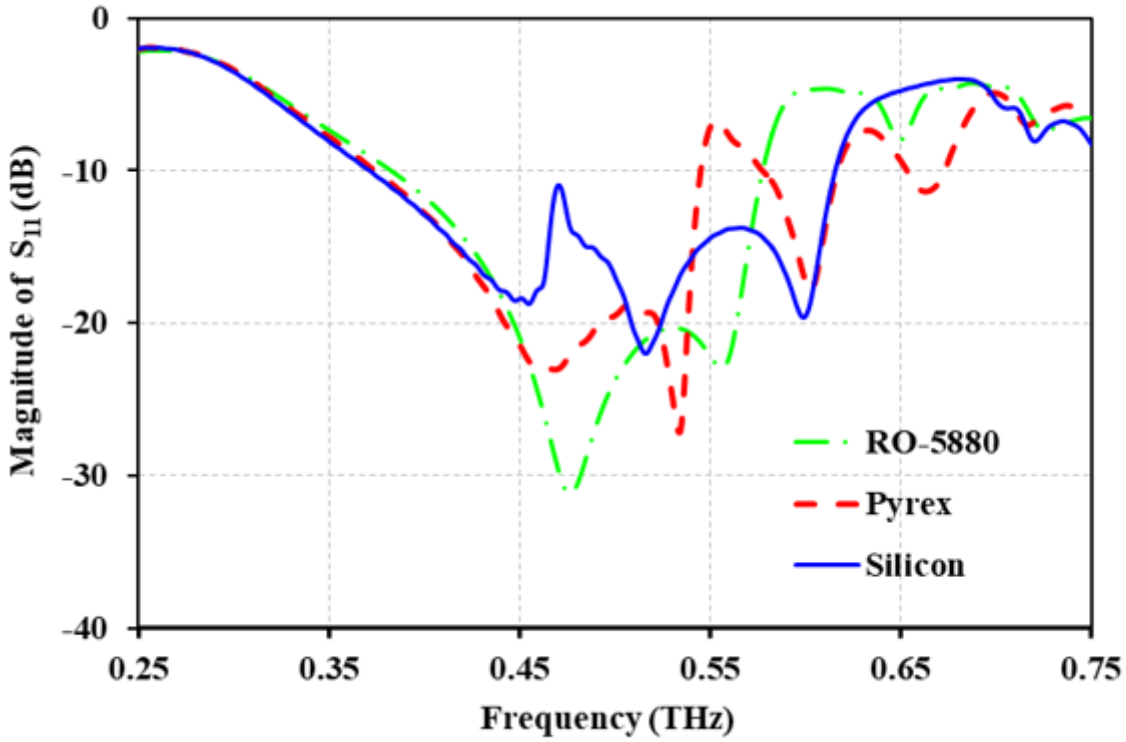

Figure 10

the material effect on return loss of the antenna investigated for Ro-5880, Pyrex and Silicon